Occurrence of liddicoatite-bearing LCT pegmatites in Sirohi region, northwest India and their rare metal potentiality

Manideepa Roy Choudhury*, Nikhil Agarwal and Suresh Chander

Geological Survey of India, Western Region, 15-16 Jhalana Dungri, Jaipur 302 004, India

Rare and trace element study of pegmatites around Sibagaon area of Sirohi region, Rajasthan, India revealed that the pegmatites are of rare element class and LCT (Li–Cs–Ta) type. Rare metal concentration in these pegmatites is notably high against crustal abundance, with Li ranging from 1007 to 10785 ppm, Rb from 1285 to 9147 ppm, Cs from 36 to 1142 ppm, Ta from 12 to 386 ppm, Sn from 54.22 to 2283.61 ppm and F from 2724 to 48,275 ppm. Integration of EPMA and LA-ICPMS analyses indicated that the main Li-bearing mineral in pegmatites is lepidolite with Li ranging from 21,599 to 28,178 ppm, which is economically worthwhile to process for Li, followed by elbaite and rare mineral liddicoatite, which has not been reported so far in India. Rare earth element (REE) distribution pattern shows enrichment of LREEs than HREEs, indicating that pegmatites are fractionated and thus causing enrichment of rare metals. This reporting of liddicoatite-bearing LCT pegmatites from Sirohi region with high anomalous values of rare metals can therefore be a good prospect for rare metal exploration in India in the present economic scenario. These pegmatites have indicated a syn-collisional signature and may be related to the accretion of Marwar craton with greater Indian land mass along the Phulad Shear zone.

Keywords: Liddicoatite, pegmatites, rare metals, trace elements.

THE Aravalli–Delhi Fold Belt in northwestern India is a NE–SW trending, long mountain chain which consists of multiply folded and polymetamorphosed rocks[1–7]. It has always been one of the prime targets for exploration of base metals, radioactive elements, rare earth elements (REEs) and rare metals[8–10]. The closing of Delhi orogeny in northwest (NW) India has led to widespread intrusion of granites and pegmatites. Pegmatites are important sources of rare metals, mainly Li, Cs, Ta, Nb and REEs[11]. The Sirohi region situated in the southwestern sector of NW India hosts widespread granitic and pegmatite bodies. Many workers in the past decades have carried out studies in this region, which were mainly focused on magmatism[12], granite geochemistry[13], granite intrusion-induced deformation[1], tungsten mineralization[12,14] and distribution pattern of radioactive elements[9]. However, detailed studies on rare metal mineralization have not received much attention.

This study presents the results of systematic geochemical characterization and potentiality of rare metals, mainly lithium, cesium and rubidium of pegmatites in the Sirohi region. Detailed geochemistry of rare metal-bearing mineral phases is also carried out along with first time reporting of the mineral liddicoatite in India. The study also compares the geochemical features and rare metal potentiality of pegmatites of Sirohi region with the world class Tanco pegmatite deposit[15] at Bernic Lake, in southeastern Manitoba, Canada.

The Sirohi region comprises of NE–SW trending ridges formed by Neoproterozoic metasediments of the Sirohi Group[2]. These are fringed on both the eastern and western sides by Erinpura granite and gneisses, and are associated with large-scale faults and shears zones[1,3,16,17] (Figure 1). Around Sibagaon area, located about 15 km towards northeast of Sirohi, a series of pegmatite bodies intruding the rocks of the Sirohi Group are present. Sirohi Group of rocks in the study area is mainly calc-silicate, quartzite, mica schist and phyllite. Pegmatites found in the area are coarse-grained, mainly composed of quartz, feldspar, lepidolite, muscovite and tourmaline (Figure 2). Pegmatites mostly maintain strike continuity with varying width. Marginal areas of pegmatites are medium to fine-grained and rich in feldspar, whereas the core is quartz-rich. Lepidolite mica is generally associated with feldspar. In most of the pegmatites tourmaline is concentrated in marginal areas, whereas in few pegmatites it is also present in the core part.

The electron probe micro analysis (EPMA) of pegmatite samples on polished thin-sections was carried out (CAMECA SX 100 electron microprobe) in the National Centres of Excellence in Geoscience Researches (NCEGR) laboratory of the Geological Survey of India (GSI) at Faridabad. Operating conditions were 15 keV accelerating voltage and probe current of 20 nA. Analyses were done using a beam diameter of 1 μm, along with all natural standards. The concentration of trace elements in different mineral phases in pegmatite on polished thin-sections was determined using Laser Ablation Inductively Coupled Plasma Mass Spectrometry (LA-ICPMS) at the LA-ICPMS Laboratory, NCEGR, Faridabad, with a CETAC Technologies 213 nm LSX G2 laser ablation unit coupled with a Agilent Technologies 7700x mass spectrometer. The LA-ICPMS was operated at 1350 W plasma power. Helium was used as the carrier gas, with a flow rate of 550 ml min^{-1} through the sample cell. Laser ablation conditions were: laser power ~2.5 Mj, with pulse frequencies 10 Hz and spot sizes of 30 μm, carrier gas flow (He + Ar) of 1.45 l min^{-1} in the ICP unit. The nebulizer flow rate was 0.9 l min^{-1}. Each analysis consisted of 60 sec of background analyses and 30 sec of ablation

*For correspondence. (e-mail: manideepa.geol@gmail.com)

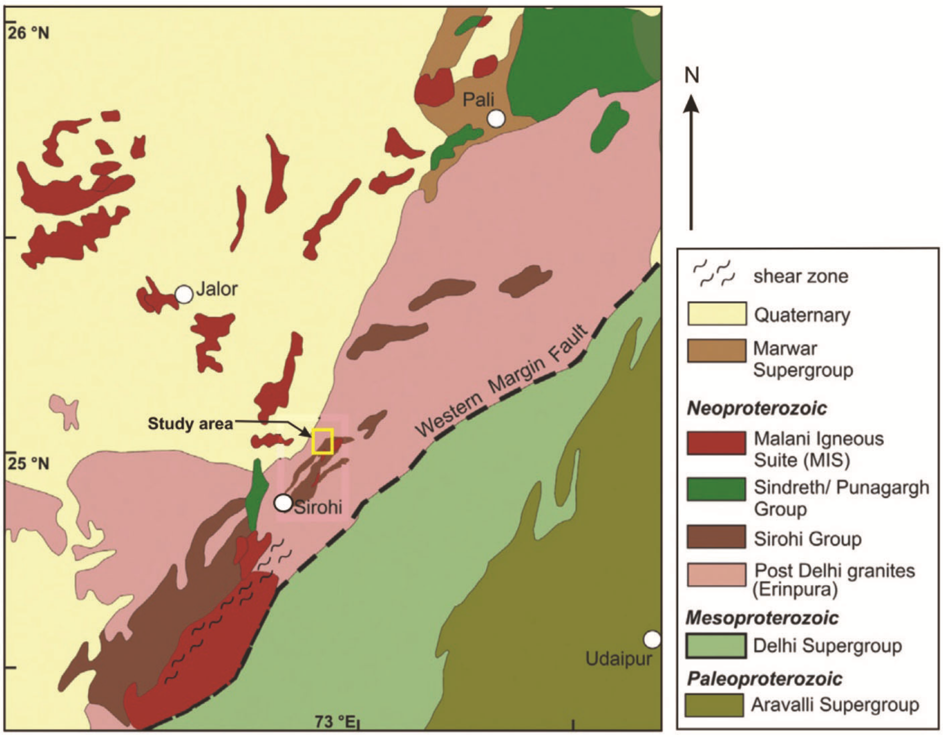

Figure 1. Geological map of Aravalli–Delhi Fold Belt (modified after Gupta *et al.*[2] and de Wall *et al.*[1]).

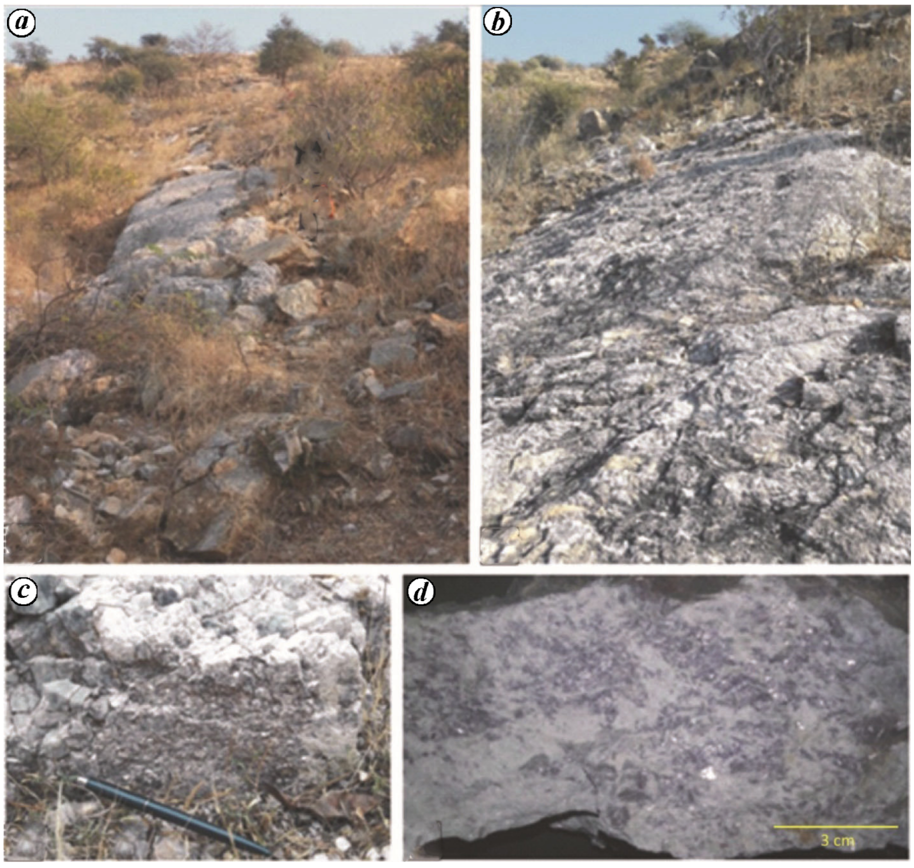

Figure 2. Field photographs showing (***a***, ***b***) pegmatites exposed in study area and (***c***, ***d***) lepidolite in pegmatites.

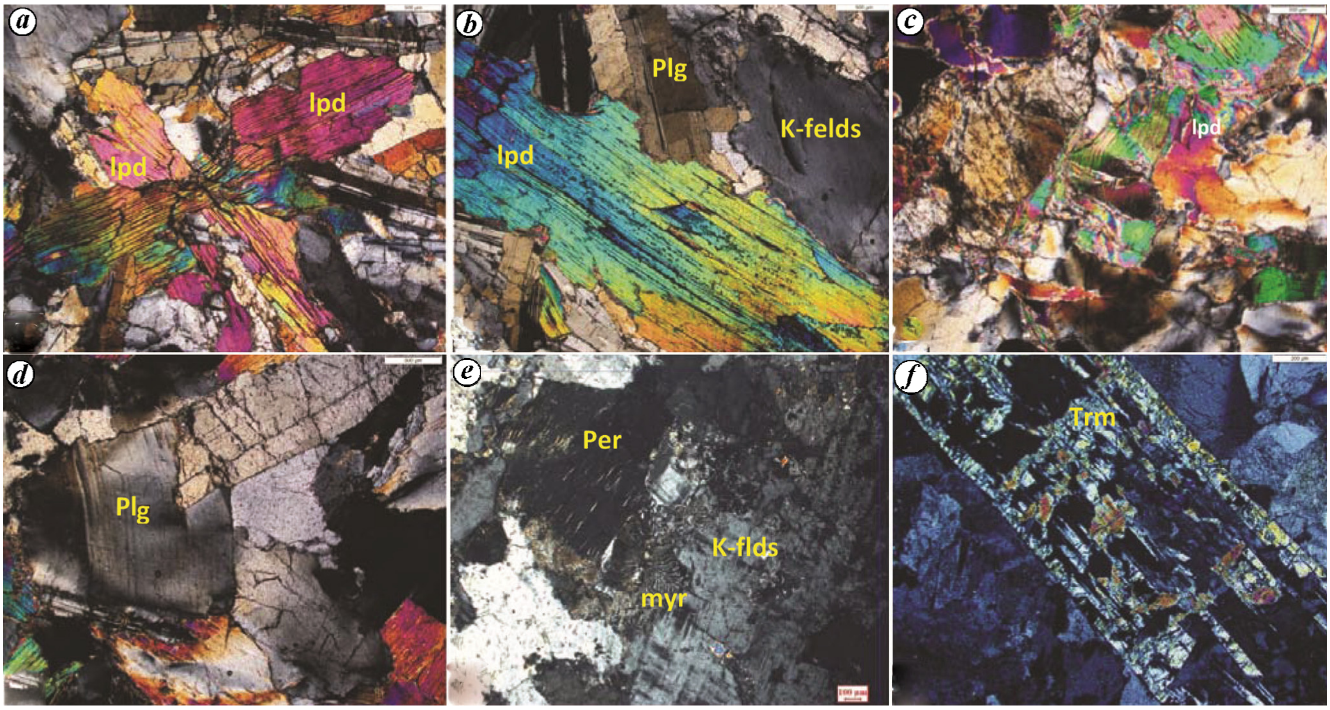

Figure 3. Photomicrographs of pegmatites showing (***a***, ***b***) coarse lepidolite (lpd), (***c***) kink bands in lepidolite, (***d***) bent twin lamellae of plagioclase feldspar (Plg), (***e***) perthite (Per) and myrmekite (myr) along the contact of potash feldspar (K-felds) and (***f***) tourmaline (Trm) being replaced by feldspar.

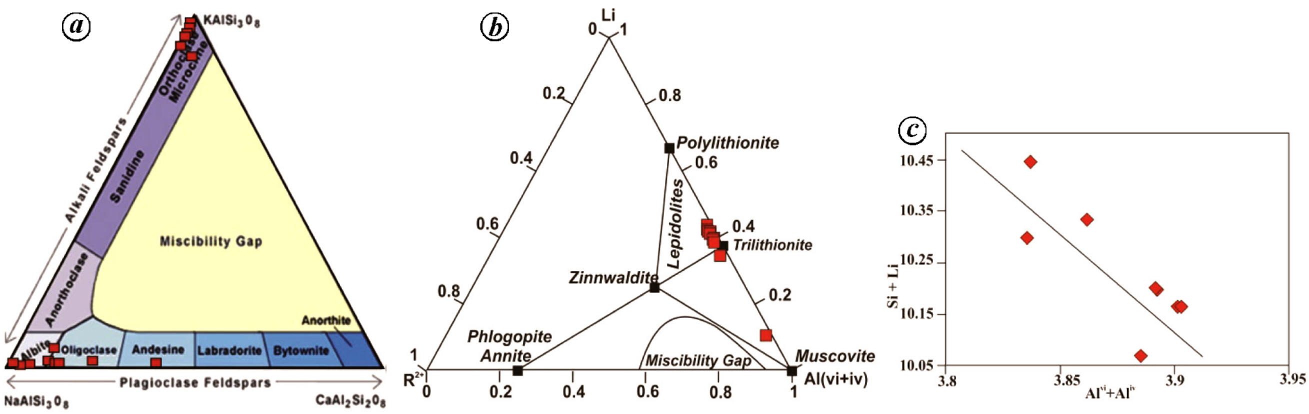

Figure 4. Geochemical plots of pegmatite showing classification of (***a***) feldspar, and (***b***) mica in Li–R^{2+}–Al diagram of Foster. (***c***) Si + Li vs Al^{vi} + Al^{iv} plot of lepidolite showing the substitution mechanism in lepidolite.

time. Data reduction was carried out using the GeoPro software (CETAC). Calibration for the analysis was carried out using NIST 610 and NIST 612 glasses as external standards[18]. Also, ^{29}Si was used as an internal standard in the analysis. The whole-rock analyses of pegmatite samples was carried out for REE and trace element concentration using Varian 800 ICPMS and Panalytical Axios XRF, at the Chemical Laboratory, Geological Survey of India, Jaipur.

Petrographic studies revealed that the pegmatites are coarse-grained showing equigranular texture with mostly euhedral to subhedral grains and consist of mainly K-feldspar, plagioclase feldspar, quartz, lepidolite mica, muscovite and tourmaline with fluorite as the accessory phase (Figure 3). Plagioclase is corroded at the margins with development of perthitic K-feldspar. At places along the grain boundary of K-feldspar, well-developed myrmekite is presently replacing K-feldspar (Figure 3 *e*).

EPMA analyses show that plagioclase composition ranges from albite to oligoclase (Figure 4 *a*). For mica, generally major and trace element composition is analysed using EPMA with limitations to detect the lightest elements such as Li, He and H, which are determined using stoichiometry. In the present study, therefore, a

Table 1. Representative analyses of micas and tourmaline by electron probe micro analysis (EPMA) with their corresponding laser ablation inductively coupled plasma mass spectrometry (LA-ICPMS) analyses. Major oxides (wt%) via microprobe, Li (ppm) and trace elements (ppm) using LA-ICPMS

EPMA analyses (wt%)								
	Lepidolite							Muscovite
Point	L1	L2	L3	L4	L5	L6	L7	L6
SiO_2	52.16	51.80	52.62	51.88	52.63	52.40	51.89	51.92
TiO_2	0.00	0.00	0.12	0.07	0.10	0.04	0.08	0.06
Al_2O_3	22.69	22.55	22.50	22.67	21.56	22.35	22.42	22.55
FeO	0.00	0.13	0.04	0.01	0.09	0.01	0.04	0.00
MnO	0.16	0.10	0.17	0.14	0.14	0.17	0.17	0.17
MgO	0.13	0.13	0.10	0.07	0.09	0.03	0.15	0.03
CaO	0.00	0.04	0.00	0.00	0.02	0.00	0.03	0.03
Na_2O	0.21	0.36	0.23	0.16	0.36	0.22	0.33	0.16
K_2O	9.74	9.88	10.00	9.99	9.65	9.89	9.78	9.87
F	8.82	8.69	8.32	8.17	8.39	8.68	8.54	9.41
Cl	0.02	0.04	0.03	0.00	0.02	0.01	0.05	0.03
P_2O_5	0.00	0.02	0.01	0.00	0.02	0.00	0.03	0.05
Total	93.91	93.73	94.12	93.16	93.06	93.78	93.51	94.27
LA-ICPMS analyses (ppm)								
Li	26,046	25,014	26,919	25,903	21,599	28,178	27,578	3164
Sc	1.67	–	0.26	1.43	1.73	1.00	0.72	31.47
Ti	259.58	97.91	144.89	195.96	208.94	199.56	137.06	–
V	0.12	1.16	0.44	0.02	–	–	0.94	196.57
Cr	5.01	18.45	4.89	2.59	–	16.95	12.90	–
Ni	–	7.97	–	0.46	–	0.06	8.88	172.67
Rb	14,428	130,620	12,994	13,961	13,009	14,204	13,457	12,509
Sr	0.18	0.31	0.18	0.24	0.32	0.94	6.11	bdl
Y	bdl	bdl	0.04	bdl	bdl	bdl	0.11	bdl
Zr	0.30	bdl	–	0.38	0.33	0.18	1.58	bdl
Nb	78.41	164.72	129.58	123.51	102.91	129.79	129.51	139.34
Sn	122.19	118.53	122.79	184.00	138.55	129.66	108.07	2616.44
Cs	1580	2880	2605	2301	3431	3170	4026	254.84
La	0.02	bdl	0.02	bdl	–	–	0.18	–
Ce	bdl	0.11	–	0.03	bdl	–	0.18	–
Pr	0.02	0.26	0.01	0.05	bdl	bdl	0.01	14.17
Nd	–	2.22	bdl	–	0.14	0.69	0.00	88.00
Sm	bdl	2.07	bdl	–	–	–	–	–
Eu	0.03	0.73	–	0.11	0.09	0.03	–	–
Gd	bdl	bdl	bdl	0.19	–	0.73	0.07	216.97
Tb	bdl	0.21	–	bdl	–	–	–	–
Dy	0.08	bdl	–	0.06	bdl	–	–	–
Ho	0.03	–	bdl	0.09	bdl	0.04	–	–
Er	0.04	1.31	0.09	0.09	bdl	bdl	–	bdl

EPMA analyses (wt%)								
	Elbaite	Liddicoatite	Liddicoatite	Liddicoatite	Elbaite	Dravite	Schorl	Elbaite
Point	T1	T2	T3	T4	T5	T6	T7	T8
SiO_2	37.09	38.20	37.61	35.97	35.17	36.91	37.79	37.46
TiO_2	0.00	0.12	0.15	0.13	0.16	0.39	0.10	0.21
Al_2O_3	37.68	36.58	37.77	35.34	36.27	35.38	37.88	34.58
Fe_2O_3	0.42	0.35	0.41	0.34	0.48	0.14	0.58	0.60
FeO	2.29	1.93	2.23	1.86	2.64	0.78	3.18	3.31
MnO	0.13	0.17	0.15	0.14	0.12	0.20	0.15	0.08
MgO	0.68	0.66	0.40	0.41	3.52	6.75	0.77	4.88
CaO	2.53	3.14	2.94	3.06	0.62	1.79	2.53	1.45
Na_2O	1.37	1.23	1.16	1.15	2.23	1.68	1.55	1.82
K_2O	0.06	0.05	0.05	0.07	0.03	0.02	0.01	0.04
F	1.60	1.48	1.50	1.46	0.99	0.88	1.31	1.65
Cl	0.02	0.03	0.02	0.03	0.01	0.00	0.00	0.00
B_2O_3	10.76	10.785	10.8	10.15	10.56	10.86	10.814	11.01
H_2O*	2.62	2.57	2.49	2.09	2.28	3.07	2.35	2.39
Total	97.25	97.29	97.67	92.17	95.08	98.83	99.01	99.49
LA-ICPMS analyses (ppm)								
Li	7572	7114	6162	3373	7266	3608	2171	10902
Sc	0.53	0.82	0.71	7.05	6.24	15.28	2.06	2.69
Ti	258.33	371.08	391.69	542.11	3298	4418	160.42	1606
V	7.55	4.73	11.49	13.39	106.83	142.45	4.09	41.42
Cr	151.96	26.13	4.92	616.75	0.87	159.74	12.15	17.68
Ni	0.12	0.52	1.46	5.39	6.62	33.85	1.45	5.45
Rb	0.01	0.21	1.05	1035.02	0.08	1.34	856.99	0.09
Sr	98.98	101.78	69.99	261.82	63.76	43.32	110.19	186.09
Y	bdl	0.02	0.07	6.47	0.12	0.02	1.28	0.12
Zr	bdl	0.17	2.06	140.50	–	0.88	35.95	0.10
Nb	3.67	2.62	1.49	3.97	5.69	1.64	0.86	3.53
Sn	62.89	40.22	33.23	90.30	136.39	107.17	17.13	154.42
Cs	–	0.14	0.14	161.10	1.66	0.58	72.09	0.02
La	11.78	8.65	7.60	15.43	21.71	10.87	5.79	40.62
Ce	18.73	14.13	10.20	27.08	39.13	20.90	9.18	79.96
Pr	1.71	1.49	0.90	3.39	3.47	1.92	0.96	7.63
Nd	3.52	4.05	3.38	5.25	12.19	8.28	4.38	28.68
Sm	0.17	0.17	0.18	2.13	0.64	0.60	0.13	3.13
Eu	0.11	0.29	0.09	0.99	0.24	0.23	0.29	1.23
Gd	0.13	–	–	–	0.36	0.37	0.94	0.27
Tb	0.02	0.01	0.03	0.25	bdl	0.01	0.16	–
Dy	bdl	bdl	–	–	0.21	0.10	0.29	0.33

(*Contd*)

Table 1. (*Contd*)

	LA-ICPMS analyses (ppm)							
	Lepidolite							Muscovite
Tm	–	–	–	bdl	–	–	bdl	bdl
Yb	–	–	0.27	0.15	0.12	–	0.12	–
Lu	0.03	–	0.09	bdl	0.04	–	–	bdl
Ta	20.1	50.72	36.1	39.5	37.3	36.8	39.6	53.8
Th	bdl	–	0.01	0.05	0.04	0.14	0.01	bdl
U	–	0.17	–	–	–	0.20	–	6.78
apfu								
Si^{4+}	7.59	7.57	7.61	7.57	7.70	7.63	7.58	7.59
Ti^{4+}	0.00	0.00	0.01	0.01	0.01	0.00	0.01	0.01
Al^{3+}	3.89	3.89	3.84	3.90	3.72	3.84	3.86	3.88
Fe^{2+}	0.00	0.02	0.00	0.00	0.01	0.00	0.01	0.00
Mn^{2+}	0.02	0.01	0.02	0.02	0.02	0.02	0.02	0.02
Ni^{2+}	0.00	0.00	0.00	0.00	0.00	0.00	0.00	0.00
Mg^{2+}	0.03	0.03	0.02	0.02	0.02	0.01	0.03	0.01
Ca^{2+}	0.00	0.01	0.00	0.00	0.00	0.00	0.00	0.00
Ba^{2+}	0.00	0.00	0.00	0.00	0.00	0.00	0.00	0.00
Na^{+}	0.06	0.10	0.06	0.05	0.10	0.06	0.09	0.04
K^{+}	1.81	1.84	1.84	1.86	1.80	1.84	1.82	1.84
Al^{iv}	0.41	0.43	0.39	0.43	0.30	0.37	0.42	0.41
Al^{vi}	3.48	3.45	3.44	3.47	3.42	3.47	3.44	3.47

	LA-ICPMS analyses (ppm)							
	Elbaite	Liddicoatite	Liddicoatite	Liddicoatite	Elbaite	Dravite	Schorl	Elbaite
Ho	–	0.02	bdl	0.56	0.01	–	0.12	0.01
Er	0.01	–	0.02	2.52	bdl	0.08	0.12	0.22
Tm	–	–	–	0.12	0.03	–	0.13	0.02
Yb	0.06	0.00	0.19	1.61	–	–	0.28	0.04
Lu	–	–	0.06	–	0.01	bdl	bdl	–
Ta	0.77	0.56	2.1	9.1	0.94	1.7	0.6	6.01
Th	0.15	0.05	0.63	12.72	0.04	0.04	1.96	1.21
U	–	–	0.03	1.96	–	0.04	0.35	0.01
apfu								
Si	5.99	6.16	6.05	6.16	6.07	5.79	5.91	5.91
Ti	0.00	0.01	0.02	0.02	0.01	0.02	0.05	0.02
Al	7.17	6.95	7.16	7.13	7.18	7.04	6.67	6.43
Fe^{3+}	0.05	0.04	0.05	0.04	0.07	0.06	0.02	0.07
Fe^{2+}	0.31	0.26	0.30	0.27	0.43	0.36	0.10	0.44
Mn^{2+}	0.02	0.02	0.02	0.02	0.02	0.02	0.03	0.01
Mg	0.16	0.16	0.10	0.11	0.18	0.87	1.61	1.15
Ca	0.44	0.54	0.51	0.56	0.44	0.11	0.31	0.25
Na	0.43	0.39	0.36	0.38	0.48	0.71	0.52	0.56
K	0.01	0.01	0.01	0.02	0.00	0.01	0.00	0.01
Fe^{2+}(Y)	0.31	0.26	0.30	0.27	0.43	0.36	0.10	0.44
Mg(Y)	0.16	0.16	0.10	0.11	0.18	0.87	1.61	1.15
Li(Y)	1.06	0.99	0.86	0.50	0.30	1.04	0.50	1.49
X-vacancy	0.12	0.06	0.12	0.04	0.08	0.17	0.17	0.19

bdl, Below detection limit; H_2O*, Calculated from stoichiometric constraints.

Table 2. Classification of pegmatites of Sibagaon area, Sirohi district, Rajasthan, India

Typical minor elements with geochemical signatures (ppm)	Pegmatite type and family	Significant feature
Li – 1007 to 10,785 (average 2878) Rb – 1285 to 9147 (average 3871) Cs – 36 to 1142.41 (average 295) Sn – 54.22 to 2283.61 (average 548.83) Be – 6 to 822 (average 145) Ta – 12 to 386 (average 86) Nb – 19 to 132 (average 47), Ta > Nb F – 2724 to 48275 (average 14593) P – 50 to 1528	REL class, LCT family[24]	Very fertile

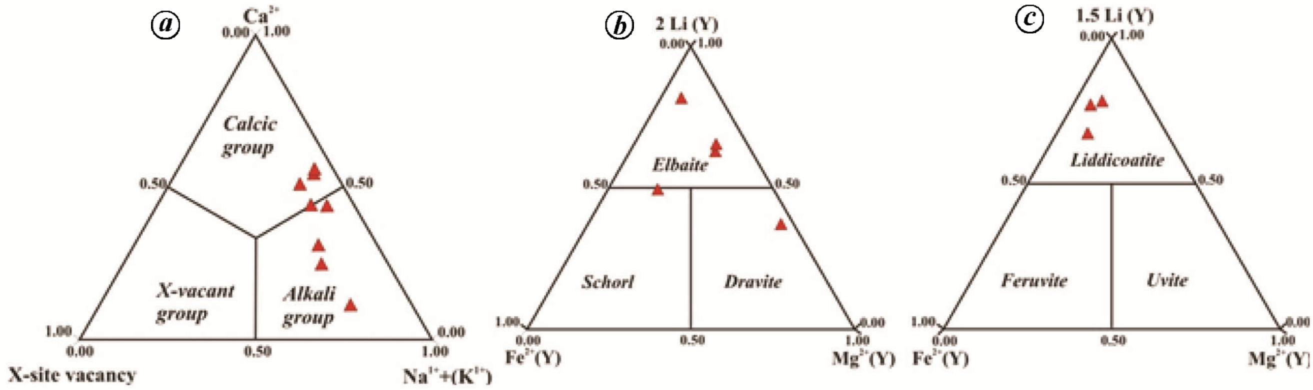

Figure 5. Classification of tourmaline from pegmatites of the study area. ***a***, Ternary classification based on dominant occupancy of the *X*-site. ***b***, Ternary classification of alkali group of tourmalines. ***c***, Ternary classification of calcic group of tourmalines.

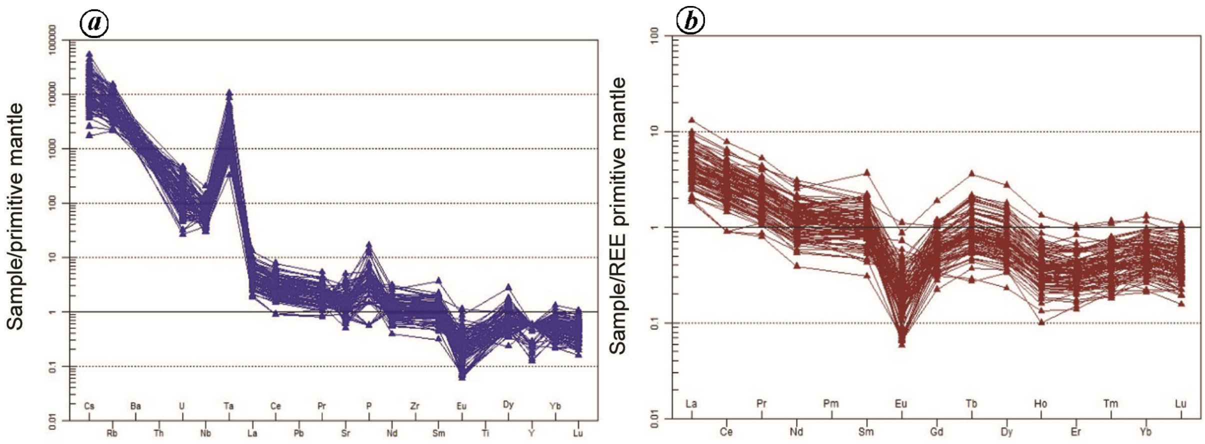

Figure 6. (***a***) Primitive mantle-normalized multi-element plots and (***b***) primitive mantle-normalized REE plots for pegmatites of the study area. Normalizing factors from McDonough and Sun[36].

combination of EPMA and LA-ICPMS was used for mica analyses (Table 1). The ternary R^{3+}–Li–R^{2+} diagram[19] (Figure 4 *b*) shows that most of the micas are lepidolite, with a few muscovite. LA-ICPMS analyses indicate that Li in lepidolite ranges from 21,599 to 28,178 ppm. The main substitution mechanisms which operated in lepidolite is $2Si + Li \leftrightarrow 3Al^{total}$ indicated by an inverse relation between the Si + Li vs $Al^{vi} + Al^{iv}$ plot (Figure 4 *c*). This is in agreement with the findings of mica from the Tanco pegmatite deposit[15,20], which also contains lepidolite showing the same substitution mechanism. For tourmaline analyses also, a combination of EPMA and LA-ICPMS analyses was used. Tourmaline structural formula was calculated using winTcac programme[21]. Table 1 provides the representative analyses of tourmaline. Based on X-site occupancy classification[22], tourmaline from pegmatites of the study area belongs principally to the alkali group and a few to the calcic group (Figure 5 *a*). The

Table 3. Chemical whole-rock analyses of pegmatites showing REE and trace element concentration (ppm) of representative samples

Sample	P	Nb	Rb	Sr	Li	Cs	F	Be	Ge	Y	Sn	La	Ce	Pr	Nd	Sm	Eu	Gd	Tb	Dy	Ho	Er	Tm	Yb	Lu	Ta	U
S-1	262	50	7081	40	7657.14	429.04	12240.00	35.37	5.19	2.50	473.71	2.35	4.68	0.47	1.35	0.47	0.02	0.37	0.12	0.67	0.07	0.17	0.03	0.20	0.02	36.45	0.64
S-2	262	57	6606	34	4539.62	502.50	14120.00	9.20	5.15	2.50	837.45	1.91	3.17	0.30	0.81	0.21	0.03	0.19	0.05	0.28	0.04	0.10	0.02	0.13	0.02	76.65	1.85
S-3	349	29	4251	31	1370.28	194.45	11044.00	10.58	25.07	2.50	206.46	1.90	3.40	0.36	1.08	0.36	0.03	0.26	0.09	0.47	0.06	0.14	0.03	0.19	0.02	35.43	1.10
S-4	218	63	8118	34	9548.64	534.67	18300.00	317.65	6.29	2.50	637.97	1.61	3.17	0.31	0.94	0.30	0.02	0.25	0.07	0.40	0.04	0.11	0.02	0.14	0.02	74.99	1.77
S-5	218	61	8890	32	6353.08	578.63	26320.00	408.77	12.50	2.50	129.91	2.36	4.32	0.49	1.56	0.49	0.03	0.35	0.10	0.57	0.06	0.15	0.03	0.16	0.02	68.97	1.58
S-6	218	67	6306	31	8027.04	434.18	16028.00	9.34	5.88	2.50	255.26	1.61	2.68	0.27	0.86	0.22	0.03	0.18	0.05	0.25	0.03	0.09	0.02	0.12	0.02	134.18	3.74
S-7	218	71	9147	43	10785.54	541.98	23572.00	97.25	5.77	2.50	270.09	1.88	3.32	0.35	1.03	0.35	0.02	0.26	0.08	0.46	0.05	0.13	0.03	0.16	0.02	108.07	2.83
S-8	262	50	5075	37	5818.56	384.24	15012.00	17.63	6.62	2.50	453.88	2.14	3.80	0.39	1.21	0.33	0.04	0.28	0.08	0.45	0.06	0.15	0.03	0.20	0.02	50.00	1.30
S-9	306	59	8385	36	10682.36	567.45	23640.00	15.94	6.89	2.50	306.66	1.36	2.43	0.26	0.73	0.24	0.02	0.18	0.06	0.32	0.03	0.08	0.01	0.10	0.01	50.09	0.97
S-10	349	50	4280	33	4739.20	491.13	12864.00	717.23	22.71	2.50	2283.61	2.98	5.06	0.49	1.56	0.34	0.06	0.30	0.07	0.45	0.07	0.16	0.04	0.27	0.03	99.34	3.06
S-11	349	46	4792	36	2655.74	363.35	12624.00	175.46	8.25	2.50	176.03	2.22	4.19	0.41	1.17	0.40	0.03	0.32	0.10	0.56	0.06	0.14	0.03	0.19	0.02	91.73	2.93
S-12	306	44	3883	31	2874.90	261.69	14520.00	8.52	14.53	2.50	424.29	1.77	2.95	0.30	0.92	0.24	0.03	0.21	0.05	0.30	0.03	0.10	0.02	0.13	0.01	97.94	3.48
S-13	262	69	6059	30	4117.18	450.33	21080.00	10.94	12.82	2.50	112.25	2.00	3.98	0.43	1.49	0.40	0.05	0.31	0.08	0.41	0.06	0.16	0.03	0.18	0.02	144.23	5.36
S-14	480	72	5084	53	2555.56	649.19	14640.00	250.37	7.82	2.50	576.21	2.41	4.09	0.42	1.24	0.40	0.04	0.30	0.09	0.49	0.06	0.14	0.03	0.22	0.03	167.73	4.39
S-15	436	51	4289	33	3077.24	573.61	12288.00	180.42	10.98	2.50	479.58	2.06	3.63	0.37	1.06	0.37	0.02	0.28	0.08	0.47	0.05	0.14	0.03	0.24	0.03	77.60	2.21
S-16	349	66	5130	31	3428.94	793.45	16360.00	68.20	8.21	2.50	395.53	1.70	3.08	0.32	0.89	0.31	0.02	0.23	0.07	0.39	0.04	0.12	0.02	0.14	0.02	75.23	5.11
S-17	524	76	6196	41	2995.30	909.24	16744.00	822.13	8.61	2.50	241.07	2.22	3.71	0.45	1.35	0.41	0.04	0.31	0.10	0.49	0.06	0.14	0.03	0.22	0.03	111.07	2.72
S-18	480	57	2087	99	1082.99	168.45	20480.00	53.70	6.75	2.50	211.88	2.20	3.29	0.32	1.03	0.23	0.08	0.18	0.05	0.27	0.04	0.11	0.02	0.16	0.02	155.79	4.44
S-19	1528	132	5563	61	3325.13	444.38	20040.00	55.21	25.10	2.50	1240.98	6.09	10.50	1.06	3.51	0.73	0.17	0.55	0.12	0.66	0.08	0.24	0.05	0.33	0.04	385.55	8.86
S-20	349	73	3752	39	3164.96	621.18	14000.00	700.36	11.96	2.50	2172.47	2.20	4.12	0.41	1.12	0.17	0.06	0.17	0.03	0.16	0.02	0.06	0.01	0.11	0.01	125.62	2.79
S-21	524	58	6607	35	6410.56	742.06	15920.00	40.67	8.51	2.50	441.46	5.61	7.69	0.72	1.89	0.46	0.06	0.37	0.09	0.53	0.06	0.17	0.03	0.26	0.03	38.52	1.37
S-22	1135	80	1366	72	1656.00	77.00	3356.00	145.28	6.33	1.14	367.38	2.22	3.54	0.40	1.35	0.32	0.09	0.24	0.06	0.34	0.04	0.14	0.03	0.14	0.03	221.53	5.91
S-23	436	48	1803	34	1515.00	230.00	3600.00	549.26	6.56	0.99	70.91	1.94	3.86	0.28	0.94	0.19	0.05	0.19	0.03	0.23	0.02	0.09	0.02	0.10	0.02	116.13	4.46
S-24	1047	61	1285	20	1623.00	36.00	4200.00	539.09	5.88	2.50	241.61	3.82	4.96	0.61	1.97	0.52	0.05	0.38	0.11	0.55	0.08	0.20	0.03	0.25	0.04	160.81	4.26
S-25	698	95	3117	31	2016.00	511.00	10714.29	68.50	9.83	2.50	296.79	4.64	5.62	0.58	1.71	0.40	0.04	0.35	0.08	0.37	0.05	0.14	0.03	0.19	0.03	322.60	8.29
S-26	262	35	1991	34	1465.00	205.00	5000.00	19.48	7.00	2.50	474.87	1.27	1.50	0.28	0.86	0.27	0.02	0.23	0.06	0.29	0.03	0.08	0.01	0.09	0.02	81.66	2.52
S-27	306	27	2999	16	2089.00	178.00	7960.00	410.84	21.93	2.08	329.27	4.02	7.88	1.05	3.84	0.89	0.07	0.65	0.14	0.73	0.10	0.27	0.04	0.40	0.05	24.12	2.24
S-28	175	32	3234	17	2013.00	177.00	6080.00	10.32	10.79	0.58	310.81	3.54	5.74	0.59	1.61	0.41	0.02	0.27	0.06	0.30	0.03	0.10	0.02	0.14	0.02	45.74	1.80
S-29	175	24	1727	12	1662.00	98.00	5480.00	72.44	22.91	0.71	394.28	4.63	7.36	0.75	2.17	0.57	0.02	0.38	0.08	0.40	0.04	0.11	0.02	0.21	0.03	79.12	4.43
S-30	50	64	1774	16	1812.00	104.00	5520.00	324.69	8.35	0.98	879.16	4.96	7.82	0.76	2.57	0.54	0.05	0.49	0.09	0.27	0.07	0.27	0.04	0.33	0.04	82.35	2.23
S-31	50	20	2375	15	1944.00	123.00	8280.00	190.13	18.85	0.81	455.62	2.91	4.75	0.47	1.31	0.33	0.01	0.24	0.05	0.28	0.04	0.10	0.02	0.16	0.02	23.96	1.96
S-32	131	69	2485	12	2070.00	165.00	6560.00	53.82	6.57	1.23	420.08	5.36	8.80	0.86	2.53	0.54	0.03	0.43	0.07	0.44	0.06	0.20	0.04	0.40	0.05	126.16	7.50
S-33	175	42	3172	13	2084.00	147.00	6520.00	72.05	10.21	0.53	350.98	4.67	7.70	0.78	2.01	0.46	0.01	0.34	0.06	0.34	0.04	0.10	0.02	0.15	0.02	88.64	3.97
S-34	131	22	2760	14	2119.00	189.00	6960.00	68.38	8.55	1.00	730.38	4.09	6.91	0.68	1.82	0.46	0.02	0.33	0.08	0.48	0.06	0.17	0.03	0.25	0.03	64.17	3.24
S-35	306	52	1347	10	1451.00	54.00	4160.00	13.49	15.58	1.85	1464.97	1.93	3.93	0.33	0.98	0.39	0.03	0.29	0.09	0.48	0.06	0.13	0.03	0.20	0.02	188.24	9.25
S-36	131	25	3503	16	1800.00	120.00	4640.00	56.13	6.74	1.04	345.81	2.21	3.61	0.40	1.22	0.31	0.03	0.23	0.05	0.31	0.05	0.14	0.03	0.27	0.04	65.63	5.00
S-37	131	31	4059	20	2116.00	278.00	9320.00	29.14	11.02	0.99	751.56	3.49	6.09	0.64	1.94	0.40	0.03	0.29	0.06	0.45	0.05	0.19	0.03	0.25	0.03	48.70	2.27
S-38	50	27	3736	18	2123.00	201.00	9040.00	32.08	10.10	1.11	717.46	2.69	4.78	0.49	1.54	0.36	0.03	0.29	0.07	0.45	0.06	0.20	0.04	0.39	0.06	32.62	2.55
S-39	175	23	2507	31	2538.00	115.00	8377.76	18.01	3.31	2.50	135.58	1.19	1.50	0.20	0.48	0.12	0.01	0.16	0.04	0.24	0.03	0.07	0.01	0.12	0.03	12.03	<0.50
S-40	262	45	6457	32	2169.00	388.00	27882.96	60.59	6.73	2.50	340.97	3.28	6.30	0.68	2.24	0.67	0.04	0.45	0.14	0.86	0.09	0.36	0.05	0.36	0.04	49.61	1.60
S-41	50	33	3066	26	1818.00	107.00	6235.29	58.06	7.03	2.50	190.87	5.15	8.06	0.82	2.51	0.51	0.02	0.35	0.08	0.41	0.05	0.20	0.04	0.37	0.05	46.09	2.24
S-42	131	28	2313	20	1945.00	137.00	19072.16	10.73	15.18	2.50	356.92	3.84	6.80	0.66	1.74	0.53	0.01	0.41	0.13	0.63	0.06	0.17	0.03	0.30	0.04	59.13	3.66
S-43	349	26	3013	24	2024.00	151.00	12886.60	107.46	11.03	2.50	160.13	2.37	3.98	0.51	1.39	0.54	0.03	0.27	0.11	0.62	0.06	0.16	0.01	0.24	0.03	67.10	3.25
S-44	262	27	2872	24	1808.00	146.00	15155.62	26.46	13.09	2.50	603.62	4.22	7.06	0.79	2.11	0.56	0.02	0.46	0.12	0.58	0.09	0.29	0.03	0.36	0.05	54.87	3.56
S-45	131	36	2594	22	2005.00	113.00	14780.60	92.04	9.28	2.50	354.97	1.98	2.78	0.31	0.67	0.19	0.01	0.12	0.04	0.24	0.01	0.07	0.02	0.16	0.03	25.64	0.62

(*Contd*)

Table 3. (*Contd*)

Sample	P	Nb	Rb	Sr	Li	Cs	F	Be	Ge	Y	Sn	La	Ce	Pr	Nd	Sm	Eu	Gd	Tb	Dy	Ho	Er	Tm	Yb	Lu	Ta	U
S-46	175	42	2503	18	2038.00	142.00	16274.09	301.15	6.98	2.50	392.27	1.20	1.50	0.22	0.70	0.19	0.01	0.15	0.06	0.35	0.04	0.12	0.02	0.20	0.03	42.47	1.96
S-47	131	39	2798	21	2016.00	134.00	17481.48	15.62	7.66	2.50	1177.54	3.21	5.31	0.50	1.29	0.33	0.01	0.20	0.05	0.38	0.03	0.11	0.01	0.16	0.03	50.23	1.60
S-48	131	43	4369	39	2116.00	236.00	32081.91	374.25	9.09	2.50	589.60	2.48	4.26	0.48	1.67	0.45	0.04	0.31	0.08	0.36	0.04	0.13	0.02	0.18	0.03	45.25	1.02
S-49	175	29	3160	20	2100.00	155.00	16611.30	92.47	12.76	2.50	646.10	3.37	4.82	0.53	1.43	0.38	0.01	0.30	0.09	0.53	0.05	0.16	0.03	0.28	0.03	23.65	1.12
S-50	175	33	3065	25	1985.00	189.00	16732.28	24.50	13.09	2.50	1064.00	4.12	6.28	0.77	2.61	0.70	0.03	0.56	0.16	0.87	0.09	0.24	0.05	0.42	0.07	51.62	1.98
S-51	306	47	2690	44	1841.00	88.00	17316.02	101.51	8.90	2.50	508.18	2.78	4.64	0.46	1.25	0.31	0.01	0.22	0.05	0.31	0.03	0.10	0.02	0.16	0.03	90.18	3.65
S-52	480	40	6857	61	2110.00	311.00	48275.86	43.38	5.91	2.50	1018.72	3.59	6.03	0.76	2.68	0.80	0.05	0.59	0.21	1.20	0.15	0.43	0.07	0.58	0.07	67.61	3.57
S-53	306	33	2536	22	1949.00	81.00	15292.89	75.56	10.11	2.50	533.62	3.08	5.12	0.57	1.90	0.55	0.03	0.43	0.16	0.87	0.09	0.25	0.05	0.30	0.04	54.44	2.53
S-54	131	28	2652	23	2024.00	141.00	14298.09	44.95	8.54	2.50	575.28	2.37	4.30	0.42	1.17	0.26	0.02	0.23	0.06	0.32	0.04	0.13	0.02	0.20	0.03	50.39	2.41
S-55	218	39	4088	24	2075.00	244.00	24904.21	68.87	10.23	2.50	882.36	4.32	6.73	0.66	1.45	0.50	0.01	0.29	0.07	0.36	0.04	0.14	0.03	0.25	0.03	40.75	1.13
S-56	218	33	4289	23	2013.00	140.00	21126.76	58.53	12.14	2.50	712.49	4.56	7.07	0.73	1.89	0.52	0.02	0.34	0.08	0.34	0.04	0.13	0.03	0.29	0.03	29.51	1.13
S-57	50	39	4976	23	2132.00	242.00	30051.81	95.36	11.00	2.50	1278.65	4.14	6.32	0.66	1.60	0.45	0.01	0.35	0.08	0.44	0.06	0.23	0.05	0.42	0.05	39.97	2.11
S-58	50	32	3049	18	2099.00	159.00	19206.68	19.76	12.21	2.50	883.82	4.93	7.87	0.72	1.85	0.44	0.01	0.32	0.08	0.39	0.04	0.16	0.03	0.30	0.04	36.50	2.11
S-59	175	19	2011	25	1899.00	113.00	11787.97	295.09	11.44	2.50	687.72	2.17	3.85	0.45	1.53	0.44	0.07	0.31	0.07	0.41	0.06	0.18	0.03	0.30	0.04	20.75	2.02
S-60	175	25	3374	18	2029.00	164.00	14640.00	158.46	17.88	2.50	531.97	2.77	4.38	0.42	1.20	0.31	0.01	0.23	0.06	0.34	0.04	0.12	0.03	0.21	0.03	24.97	0.52
S-61	306	43	6573	24	2135.00	380.00	28640.00	30.58	6.64	2.50	738.72	4.98	8.07	0.78	1.94	0.48	0.01	0.36	0.08	0.40	0.04	0.12	0.02	0.19	0.02	30.28	1.07
S-62	131	34	4515	21	2117.00	242.00	24120.00	154.44	8.58	2.50	748.54	6.43	10.80	0.99	2.64	0.55	0.02	0.42	0.09	0.39	0.05	0.15	0.02	0.18	0.03	34.00	0.89
S-63	50	26	4005	25	2100.00	229.00	18840.00	11.88	9.75	2.50	379.60	3.39	4.65	0.51	1.38	0.38	0.02	0.31	0.08	0.47	0.06	0.16	0.04	0.30	0.03	23.11	1.06
S-64	50	25	2163	25	1885.00	98.00	10240.00	48.99	7.33	2.50	171.92	3.26	5.07	0.56	1.52	0.33	0.02	0.24	0.06	0.28	0.04	0.11	0.02	0.16	0.02	25.71	1.35
S-65	262	42	3523	26	2025.00	148.00	15840.00	84.13	7.92	2.50	453.54	8.41	13.06	1.34	3.54	0.78	0.02	0.58	0.14	0.72	0.08	0.24	0.05	0.41	0.06	64.52	3.86
S-66	131	28	3259	21	2010.00	133.00	17720.00	36.97	13.38	2.50	597.75	4.03	6.65	0.63	1.72	0.42	0.01	0.32	0.08	0.45	0.06	0.17	0.03	0.33	0.04	28.29	1.55
S-67	393	62	2024	54	1646.00	239.00	8960.00	388.29	7.95	2.50	1016.69	2.51	4.89	0.47	1.49	0.42	0.06	0.32	0.09	0.55	0.07	0.17	0.03	0.26	0.04	162.61	6.46
S-68	349	76	4953	29	2103.00	290.00	23720.00	26.70	8.60	2.50	523.20	1.62	3.05	0.31	0.85	0.34	0.02	0.26	0.08	0.46	0.05	0.12	0.02	0.20	0.02	136.00	5.24
S-69	349	89	2410	30	1953.00	193.00	11000.00	64.55	7.30	2.50	705.63	1.58	3.06	0.30	0.93	0.25	0.03	0.20	0.07	0.36	0.04	0.12	0.03	0.21	0.02	236.34	7.74
S-70	524	27	2704	40	1903.00	275.00	11160.71	46.76	6.79	2.50	265.18	3.07	5.89	0.65	2.06	0.81	0.04	0.59	0.19	0.99	0.10	0.26	0.03	0.26	0.03	59.79	2.36
S-71	698	58	1843	43	1790.00	153.00	11520.98	472.28	9.68	2.50	539.07	3.13	5.34	0.63	1.72	0.68	0.06	0.43	0.14	0.80	0.08	0.19	0.04	0.28	0.04	196.73	8.28
S-72	349	42	3927	27	2100.00	427.00	27439.02	127.12	16.33	2.50	660.62	2.06	3.41	0.38	0.98	0.32	0.02	0.26	0.09	0.54	0.06	0.13	0.03	0.26	0.02	87.32	4.07
S-73	306	52	3425	33	1999.00	394.00	14655.17	151.31	10.50	2.50	1013.33	1.96	4.43	0.47	1.11	0.39	0.04	0.29	0.10	0.53	0.05	0.15	0.02	0.17	0.03	128.44	4.87
S-74	436	50	2137	71	1900.00	236.00	10060.36	257.97	8.66	2.50	907.57	2.68	4.29	0.47	1.47	0.41	0.05	0.28	0.09	0.45	0.06	0.18	0.03	0.26	0.03	123.63	5.67
S-75	436	58	2230	69	1906.00	181.00	16376.81	201.80	11.72	2.50	575.13	3.54	5.87	0.62	2.07	0.44	0.06	0.36	0.10	0.51	0.06	0.15	0.03	0.24	0.04	163.21	6.99
S-76	262	38	3267	61	1792.18	261.20	20800.00	198.14	7.01	2.50	130.05	1.96	4.15	0.49	1.60	0.63	0.06	0.45	0.14	0.74	0.08	0.17	0.03	0.20	0.02	39.56	1.24
S-77	175	56	2663	78	1686.80	253.37	10560.00	240.39	4.99	2.50	54.22	1.60	2.96	0.32	1.10	0.33	0.11	0.24	0.06	0.30	0.04	0.12	0.02	0.14	0.02	89.72	3.84
S-78	1222	49	3160	36	1689.65	312.49	10240.00	405.70	11.86	2.50	259.36	5.19	9.72	1.11	3.16	1.48	0.13	1.03	0.35	1.85	0.20	0.45	0.08	0.50	0.06	77.99	3.17
S-79	611	52	3557	30	3546.64	212.24	9120.00	19.34	5.75	2.50	530.24	2.81	5.19	0.59	1.80	0.62	0.03	0.45	0.15	0.76	0.08	0.20	0.03	0.23	0.03	105.08	4.77
S-80	655	34	2768	17	2276.06	285.81	11760.00	528.36	11.73	2.50	750.70	2.87	4.56	0.55	1.61	0.57	0.04	0.41	0.15	0.75	0.09	0.25	0.05	0.35	0.05	52.63	3.14
S-81	393	68	5647	45	4724.36	683.21	11000.00	238.58	8.31	2.50	591.73	2.06	3.42	0.35	0.99	0.31	0.03	0.24	0.07	0.39	0.04	0.11	0.02	0.16	0.02	106.65	2.86
S-82	306	34	1425	20	1075.52	148.62	2724.00	6.01	5.47	2.50	169.84	1.59	2.89	0.31	0.91	0.32	0.03	0.24	0.09	0.48	0.05	0.12	0.02	0.16	0.02	49.33	1.89
S-83	480	45	5467	59	6608.64	319.28	11440.00	104.63	6.35	2.50	486.99	2.65	5.03	0.56	1.55	0.63	0.02	0.45	0.16	0.87	0.08	0.20	0.03	0.23	0.03	69.88	3.03
S-84	306	57	4768	37	4614.14	407.57	9900.00	89.41	8.38	2.50	549.60	2.89	5.64	0.66	2.05	0.82	0.03	0.62	0.22	1.11	0.11	0.25	0.04	0.28	0.03	50.47	2.46
S-85	393	42	3601	20	3039.38	488.80	14080.00	139.95	6.96	2.50	707.51	3.04	6.17	0.70	2.14	0.86	0.03	0.61	0.20	1.05	0.10	0.23	0.04	0.26	0.03	96.50	4.11
S-86	262	52	7070	37	6644.66	1142.41	24480.00	137.39	14.29	2.50	554.52	2.26	4.20	0.48	1.43	0.48	0.03	0.39	0.12	0.65	0.07	0.18	0.03	0.18	0.02	73.26	1.90
S-87	306	46	5292	33	4459.08	537.57	18080.00	50.02	4.52	2.50	156.00	2.49	5.15	0.61	1.88	0.89	0.03	0.58	0.21	1.01	0.10	0.20	0.04	0.21	0.02	35.96	1.42
S-88	436	39	1807	32	1007.46	191.31	7360.00	117.37	12.80	2.50	795.88	3.05	5.93	0.69	2.18	0.80	0.04	0.58	0.19	1.00	0.11	0.24	0.04	0.30	0.04	104.26	3.66
S-89	262	36	3046	20	1340.94	223.80	7360.00	29.63	2.93	2.50	440.27	2.81	4.95	0.66	2.24	0.74	0.07	0.64	0.19	1.01	0.13	0.30	0.05	0.31	0.04	48.09	2.45
S-90	131	53	6840	32	5858.38	404.35	19000.00	57.85	5.27	2.50	951.43	1.31	2.61	0.30	1.06	0.36	0.03	0.26	0.08	0.42	0.05	0.11	0.02	0.12	0.02	78.93	1.87
S-91	480	72	3303	38	1200.76	185.64	8640.00	13.48	6.64	2.50	163.01	2.71	5.00	0.56	1.67	0.60	0.04	0.43	0.12	0.67	0.08	0.18	0.03	0.28	0.04	212.80	5.41
S-92	480	65	3255	33	2104.00	242.00	16000.00	82.98	7.53	2.50	822.98	2.57	5.23	0.59	1.95	0.77	0.02	0.54	0.18	0.94	0.09	0.25	0.04	0.29	0.03	169.09	6.91

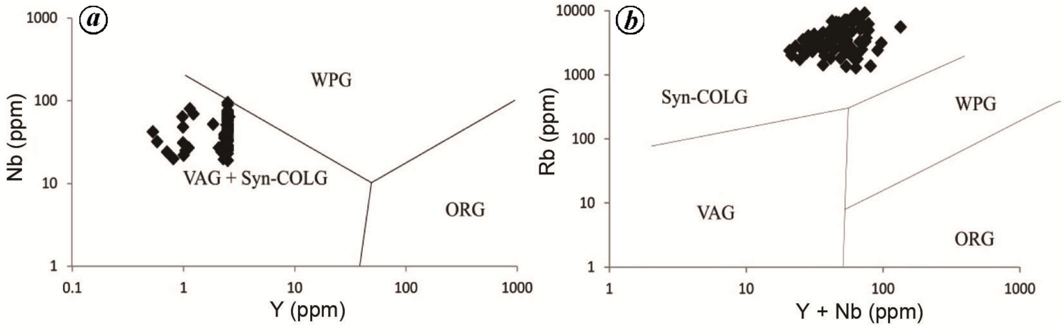

Figure 7. (***a***) Nb vs Y and (***b***) Rb vs (Nb + Y) tectonic discrimination diagrams of Pearce *et al.*[27] VAG, Volcanic arc granites; Syn-COLG, Syn-collisional granites; WPG, Within plate granites and ORG, Ocean ridge granites. The *x*-axis has been modified to accommodate low values of Y and Y + Nb in (***a***) and (***b***) respectively.

alkali group of tourmalines shows a varying range of composition and are classified from elbaite to dravite (Figure 5 *b*)[22]. Depending upon the predominance of Li^+, Fe^{2+} or Mg^{2+} on the Y-site, the calcic group of tourmalines are found to be of liddicoatite-type (Figure 5 *c*). LA-ICPMS analyses of these tourmalines show Li contents ranging from 2,171 to 10,902 ppm.

Classification of pegmatites was carried out on the basis of rare and trace element concentration (Table 2). Pegmatites were classified into rare element (REL) class[23,24]. Based on the family system of petrogenetic classification, these pegmatites were classified as LCT (Li–Cs–Ta) type[23,24], with enrichment of Li, Rb, Cs, Ta, Sn, F, P, etc. Li concentration ranged from 1,007 to 10,785 ppm, Cs ranges from 36 to 1142.41 ppm, Rb ranges from 1285 ppm to 9147 ppm and Ta ranges from 12 to 386 ppm (Table 3).

Trace element pattern of pegmatites shows relative enrichment of the light (LREEs) and middle (MREEs) rare earth elements over the heavy rare earth elements (HREEs). The REE pattern displays strong negative Eu anomalies (Figure 6 *b*) and a distinct enrichment of Cs, Rb, Nb and Ta with depletion in Sr and Ti (Figure 6 *a*). Total REE concentrations are typically <100 ppm. These rare element enrichment and depletion patterns in pegmatites of the study area are also consistent with published data for rare-metal pegmatites of the LCT family[23,25,26]. Trace element discrimination diagrams[27] show that majority of the samples plot in the VAG + syn-COLG field of Y–Nb and in syn-COLG field of (Y + Nb)–Rb diagrams (Figure 7).

Detailed mineral chemistry has shown that pegmatites of Sibagaon area, Sirohi region contain abundant lepidolite as the main lithium-bearing mineral, along with liddicoatite and elbaite. Liddicoatite is a gem mineral and is very rare due to substantial concentration of Li and Ca in it[28]. It is found in abundance at the type locality in Madagascar[28–31], and it is reported for the first time in India. The occurrence of lepidolite with 21,599 to 28,178 ppm Li in these pegmatites is also significant, as lepidolite is economically worthwhile to process for lithium[15,32,33]. Rare and trace element study indicated that pegmatites of Sirohi region are of LCT-type and REL class, with enrichment of rare metals, mainly Li, Cs, Rb and Ta (Table 3), which are of much higher concentration against their crustal abundance that is 20 ppm for Li, 3 ppm for Cs, 2 ppm for Ta and 90 ppm for Rb[34]. Pegmatites of the study area can thus be comparable with the Tanco pegmatite deposit in Canada[15,20] which is LCT-type of pegmatite with lepidolite as Li-bearing mineral and shows similar fractionation trend as well as similar enrichment of rare metals. Pegmatites of the study area therefore can be a potential target for locating important resources of rare metals in India in the present economic scenario. Rare and trace element data also show high concentration of Rb, which may be attributed to abundance of muscovite and K-feldspar. Sr and Ti depletion can be explained by fractionation of plagioclase and Ti-oxide. Negative Eu anomaly along with low concentration of Sr can also be correlated with plagioclase fractionation. Low concentration of U, Th, etc. suggests limited crustal signature. Collisional signature is depicted from trace element discrimination diagrams[27] of the pegmatites (Figure 7). This may be attributed to accretion of the greater India land mass with the Marwar Craton that took place along the terrane boundary Phulad Shear Zone[35] located towards east of Sirohi region.

1. de Wall, H., Pandit, M. K., Sharma, K. K., Schöbel, S. and Just, J., Deformation and granite intrusion in the Sirohi area, SW Rajasthan – constraints on Cryogenian to PanAfrican crustal dynamics of NW India. *Precambrian Res*., 2014, **254**, 1–18.
2. Gupta, S. N., Arora, Y. K., Mathur, R. K., Iqballuddin, P. B., Sahai, T. N. and Sharma, S. B., Lithostratigraphic map of Aravalli region. scale 1 : 1,000,000, Geological Survey of India, Calcutta, 1980.
3. Heron, A. M., Geology of Central Rajputana. *Mem. Geol. Surv. India*, 1953, **79**, 339.
4. Just, J., Schulz, B., de Wall, H., Jourdan, F. and Pandit, M. K., Monazite CHIME/EPMA dating of the Erinpuragranitoid deformation: implications for neoproterozoic tectonothermal evolution of NW India. *Gondwana Res*., 2011, **19**, 402–412.

5. Meert, J. and Pandit, M., The Archaean and Proterozoic history of Peninsular India: tectonic framework for Precambrian sedimentary basins in India. *Mem. Geol. Soc., London,* 2015, **43**, 29–54.
6. Roy, A. B. and Jakhar, S. R., *Geology of Rajasthan (Northwest India), Precambrian to Recent*, Scientific Publishers, 2002, p. 412.
7. Singh, Y. K., Waele, B. D., Karmakar, S., Sarkar, S. and Biswal, T. K., Tectonic setting of the Balaram–Kui–Surpagla–Kengora granulites of the South Delhi Terrane of the Aravalli Mobile Belt, NW India and its implication on correlation with the East African Orogen in the Gondwana assembly. *Precambrian Res*., 2010, **183**, 669–688.
8. Khandelwal, M. K., Jain, R. C., Dash, S. K., Padhi, A. K. and Nanda, L. K., Geological characteristics and ore body modeling of Rohil Uranium Deposit, District Sikar, Rajasthan. *Mem. Geol. Soc. India*, 2010, **76**, 75–85.
9. Scharfenberg, L., de Wall, H., Schöbel, S., Minor, A., Maurer, M., Pandit, M. and Sharma, K., *In situ* gamma radiation measurements in the Neoproterozoic rocks of Sirohi region, NW India. *J. Earth Syst. Sci*., 2015, **124**, 1223–1234.
10. Somani, O. P., Misra, A., Jeyagopal, A. V., Nanda, L. K. and Parihar, P. S., Radioelemental distribution in Neoproterozoic volcano-sedimentary Sindreth Basin, Sirohi District, Rajasthan and its significance. *Curr. Sci.*, 2012, **103**(3), 305–309.
11. Ercit, T. S., REE-enriched granitic pegmatites. In *Rare Element Geochemistry and Mineral Deposits* (eds Linnen, R. L. and Samson, I. M.). Geol. Assoc. Can., Short Course Notes, 2005, vol. 17, pp. 175–199.
12. Chattopadhyay, B., Mukhopadhyay, A. K., Singhai, R. K., Bhattacharjee, J. R. and Hore, R. K., Post Erinpura acid magmatism in Sirohi and its bearing on the tungsten mineralization. In Proceedings of the Symposium Metallogeny of the Precambrian, IGCP, 1982, vol. 91, pp. 115–132.
13. Naik, M. S., The geochemistry and genesis of the granitoids of Sirohi, Rajasthan, India. *J. Southeast Asian Earth Sci.*, 1993, **8**(1–4), 111–115.
14. Srivastava, P. and Sinha, A. K., Geochemical characterization of tungsten-bearing granites from Rajasthan, India. *J. Geochem. Exp.*, 1997, **60**, 173–184.
15. United Nations Commodity Trade database, 2016; http://comtrade.un.org/
16. de Wall, H., Pandit, M. K. and Chauhan, N. K., Paleosol at the Archean–Proterozoic contact in Udaipur. *Precambrian Res*., 2012, **216–219**, 120–131.
17. Pandit, M. K., de Wall, H., Daxberger, H., Just, J., Bestmann, M. and Sharma, K. K., Mafic rocks from Erinpura gneiss terrane in the Sirohi region: possible ocean floor remnants in the foreland of the Delhi Fold Belt, NW India. *J. Earth Syst. Sci*., 2011, **127**, 627–641.
18. Pearce, N. J., Perkins, W. T., Westgate, J. A., Gorton, M. P., Jackson, S. E., Neal, C. R. and Chenery, S. P., A compilation of new and published major and trace element data for NIST SRM 610 and NIST SRM 612 glass reference materials. *Geostandards Newsl.*, 1997, **21**, 115–144.
19. Foster, M. D., Interpretation of the composition of lithium micas. *US Geol. Surv. Prof. Pap*., 1960, 354-E.
20. Van Lichtervelde, M., Grégoire, M., Linnen, R., Béziat, D. and Salvi, S., Trace element geochemistry by laser ablation ICP-MS of micas associated with Ta mineralization in the Tanco pegmatite, Manitoba, Canada. *Contrib. Mineral. Petrol.*, 2008, **155**, 791–806.
21. Yavuz, F., Karakaya, N., Yildirim, D., Çelik Karakaya, M. and Kumral, M., A Windows program for calculation and classification of tourmaline-supergroup (IMA-2011). *Comput. Geosci.*, 2014, **63**, 70–87.
22. Henry, D. J., Spreadsheet for determining the tourmaline species based on an ordered distribution of elements in the tourmaline formula, 2011; http://www.minsocam.org/msa/ammin/toc/2011/MJ11_Data/Henry_p895_11_TourmalineSpecies.xls
23. Černý, P., Geochemical and petrogenetic features of mineralization in rare-element granitic pegmatites in the light of current research. *Appl. Geochem.*, 1992, **7**, 393–416.
24. Černý, P. and Ercit, T. S., The classification of granitic pegmatites revisited. *Can. Mineral.*, 2005, **43**, 2005–2026; 10.2113/gscanmin.43.6.2005.
25. Černý, P., Meintzer, R. E. and Anderson, A. J., Extreme fractionation in rare-element granitic pegmatites – selected examples of data and mechanisms. *Can. Mineral.*, 1985, **23**, 381–421.
26. Küster, D., Romer, R., Tolessa, D., Zerihun, D., Bheemalingeswara, K., Melcher, F. and Oberthür, T., The Kenticha rare-element pegmatite, Ethiopia: internal differentiation, U–Pb age and Ta mineralization. *Miner. Deposita*, 2009, **44**, 723–750.
27. Pearce, J., Harris, N. and Tindle, G. A., Trace element discrimination diagrams for the tectonic interpretation of granitic rocks. *J. Petrol.*, 1984, **25**, 956–983.
28. Dunn, P. J., Appleman, D. E. and Nelen, J. E., Liddicoatite, a new calcium end-member of the tourmaline group. *Am. Mineral.*, 1977, **62**, 1121–1124.
29. Akizuki, M., Kuribayashi, T., Nagase, T. and Kitikaze, A., Triclinic liddicoatite and elbaite in growth sectors of tourmaline from Madagascar. *Am. Mineral*., 2001, **86**, 364–369.
30. Aurisicchio, C., Demartin, F., Ottolini, L. and Pezzotta, F., Homogeneous liddicoatite from Madagascar: a possible reference material? First EMPA, SIMS and SREF data. *Eur. J. Mineral*., 1999, **11**, 263–280.
31. Dirlam, D. M., Laurs, B. M., Pezzotta, F. and Simmons, W. B., Liddicoatite tourmaline from Anjanabonoina, Madagascar. *Gems Gemol.*, 2002, **38**, 28–53.
32. Lele, A. and Bhardwaj, P., *Strategic Materials. A Resource Challenge for India*, Pentagon Press, Institute for Defence Studies and Analyses, New Delhi, 2014, p. 221, ISBN 978-81-8274-9.
33. Meshram, P., Pandey, B. D. and Mankhand, T. R., Extraction of lithium from primary and secondary sources by pre-treatment, leaching and separation: a comprehensive review. *Hydrometallurgy*, 2014, **150**, 192–208.
34. Taylor, S. R., Abundance of chemical elements in the continental crust: a new table. *Geochimi. Cosmochim. Acta*, 1964, **28**(8), 1273–1285.
35. Chatterjee, S., Roy Choudhury, M., Das, S. and Roy, A., Significance and dynamics of the Neoproterozoic (810 Ma) Phulad Shear Zone, Rajasthan, NW India: Neoproterozoic tectonism of PSZ, NW India, *Tectonics*, 2017; 10.1002/2017TC004554.
36. McDonough, W. and Sun, S. S., The composition of the Earth. *Chem. Geol*., 1995, **67**, 1050–1056.

ACKNOWLEDGEMENTS. We thank the Additional Director General, Geological Survey of India (GSI), Western Region, Jaipur for encouragement and support. We also thank officials of the Chemical Laboratory, GSI, Western Region, and EPMA and LA-ICPMS Laboratory, NCEGR, GSI, Faridabad for analytical support; Prof. Fuat Yavuz (Istanbul Technical University, Istanbul, Turkey), for discussions on the use of winTcac software and the reviewers for their critical comments that helped to improve the manuscript.

Received 14 June 2019; revised accepted 6 November 2019

doi: 10.18520/cs/v118/i5/809-818